Dynamic modeling of an air source heat pump water heater

Farouk Fardoun, Oussama Ibrahim, Assaad Zoughaib

DYNAMIC MODELING OF AN AIR SOURCE HEAT PUMP WATER HEATER

Farouk Fardoun, Associate Professor, Department of Industrial Engineering and Maintenance, University Institute of Technology, Doctorate School of Science and Technology, Lebanese University, Saida/Lebanon

Oussama Ibrahim, PHD Student, Doctorate School of Science and Technology, Lebanese University, Beirut/Lebanon

Assaad Zoughaib, Associate Professor, Ecole des Mines de Paris, Center for Energy and Processes, Paris/France

Abstract: This paper presents a dynamic simulation model to predict the performance of an air source heat pump water heater (ASHPWH). The mathematical model consists of submodels of the basic system components i.e. evaporator, condenser, compressor, and expansion valve. These submodels were built based on fundamental principles of heat transfer, thermodynamics, fluid mechanics, empirical relationships and manufacturer's data as necessary. The model simulation was carried out using MATLAB software. Refrigerant R134a with two different reservoir volumes 150L & 200L are investigated. Additionally, different ambient air temperatures are considered. Results show that the rate of hot water production increases as the water reservoir volume decreases and the integrated COP increases as the ambient temperature increases.

Key Words: Heat pump; Dynamic modeling; Water heating; Simulation

1   INTRODUCTION

In Mediterranean countries such as Lebanon, electric water heaters are often used to generate hot water. Electric water heaters are usually simple, but not desirable in view of energy efficiency since the overall efficiency, in converting a potential energy of fossil fuels into electric energy and then into thermal energy, is quite low. Compared to those water heaters, heat pump water heating systems can supply much more heat just with the same amount of electric input used for electric water heaters.

The ASHPWH absorbs heat from the ambient air and injects it into a water storage reservoir. The use of an air source heat pump (ASHP) leads to a high sensibility of the performance to the local ambient temperature. Moreover, reaching low ambient temperatures close to 0°C, and even below, presents the disadvantage of frost formation on the evaporator, and leads to higher technical complexity due to the required defrosting. The cost of a simple ASHP (with no defrost system) is much lower, which is an advantage permitting a higher interest of this technology in developing countries.

According to a UNDP (UNDP 2005) study concerning climatic zoning for buildings in Lebanon, Lebanon was divided into four climatic zones; Zone 1: Coastal, Zone 2: Western Mid-Mountain, Zone 3: Inland Plateau, and Zone 4: High Mountain. Five weather files were created based on data from five meteorological stations (Beirut & Bayssour for zone 1, Qartaba for zone 2, Zahle for zone 3, Cedars for zone 4). Two files were created for the zone 1, since this zone has the highest population density. Based on these weather files, it was observed that during the winter season (Jan., Feb., March), the ambient temperature doesn't fall below zero in zones 1 & 2 on the contrary of zones 3 & 4. These investigations show that

a simple ASHP could be an interesting alternative to electrical water heaters for zones 1 & 2 in Lebanon (covering about 80% of the population).

Therefore, this paper presents a dynamic model of a simple ASHPWH that is used to assess its seasonal performance in the Lebanese context.

Several dynamic models of heat pumps have been developed, but few of them dealt with heat pump water heaters. Chi and Didion (Chi and Didion 1982) developed a model using a moving boundary-lumped parameter formulation for a residential air-to-air heat pump system. The momentum equation was also included in the heat exchanger models. MacArthur and Grald (MacArthur and Grald 1989) presented a model of vapor-compression heat pumps. The heat exchangers were modeled with detailed distributed formulations, while the expansion device was modeled as a simple fixed orifice. Fu et al. (Fu et al. 2003) presented a dynamic model of air-to-water dual-mode heat pump with screw compressor having four-step capacities. The dynamic responses of adding additional compressor capacity in step-wise manner were studied. Kima et al. (Kima et al. 2004) presented a dynamic model of a water heater system driven by a heat pump, finite volume method was applied to describe the heat exchangers, and lumped parameter models were used to analyze the compressor and the hot water reservoir, where dynamic simulations were carried out for various reservoir sizes. Rasmussen and Alleyne (Rasmussen and Alleyne 2006) developed an air to air heat pump system using moving boundary-lumped parameter approach for the heat exchangers. Techarungpaisan et al. (Techarungpaisan et al. 2007) presented a steady state simulation model to predict the performance of a small split type air conditioner with integrated water heater. The model used a rotary compressor and a capillary tube.

2 MATHEMATICAL MODEL

The typical ASHPWH used in this study is shown in figure 1. It is composed of the major components of the heat pump system, namely compressor, evaporator, condenser and throttling device in addition to a hot water reservoir. Static models are chosen to simulate the actuator components, since the dynamics of compressors or expansion devices are generally faster than those of the heat exchangers, where the compressor is considered as an adiabatic reciprocating one and the throttling device is considered as an electronic expansion valve. Concerning the heat exchangers, lumped parameter, moving boundary dynamic models are chosen. The modeled evaporator is a tube and fins heat exchanger type, while a shell and tube heat exchanger is chosen for the condenser, where the refrigerant flows inside the tubes.
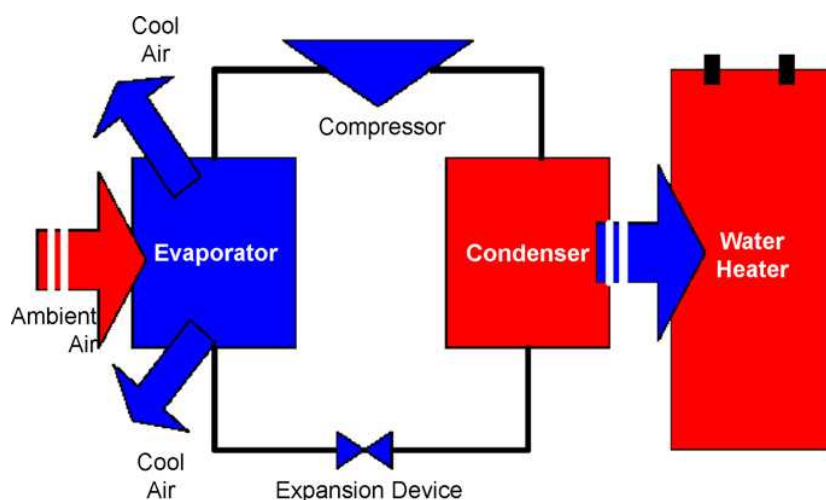

Figure 1: Air source heat pump water heater

Nomenclature

List of symbols

Variable	Explanation	Unit
A	Area	m^2
$\boldsymbol{\alpha}$	Convective heat Transfer Coefficient	$w/m^2.k$
Cp	Specific Heat	$J/kg.k$
η	Efficiency	-
COP	Coefficient of performance	-
$\bar{\boldsymbol{\gamma}}$	Mean Void Fraction	-
h	Enthalpy	J/kg
e	Internal energy	J/kg
L	Length	m
$\dot{\mathbf{m}}$	Mass Flow Rate	kg/s
P	Pressure	Pa
p	Perimeter	m
Q	Heat	w
$\boldsymbol{\rho}$	Density	kg/m^3
$\mathbf{w, u}$	velocity	m/s
T	Temperature	K
dt	Time step	s
g	Gravitational acceleration	m/s^2
k	Thermal conductivity	$w/m.k$
$\boldsymbol{\beta}$	Coefficient of thermal expansion	$1/k$
$\boldsymbol{\mu}$	Dynamic viscosity	$Pa.s$
D	Diameter	m
$\mathbf{w_k}$	Speed of compressor	rps

Subscripts

Variable	Explanation
1,2,3	$1^{st}, 2^{nd}, 3^{rd}$ Region
a	Air
e	Evaporator
c	Condenser
cs	Cross section
f	Saturated liquid
g	Saturated gas
i	Inner, inside
int	Intermediate
k	Compressor
o.out	Out
R	Refrigerant
v	Valve, volumetric
w	Wall
wat	Water
s	Saturated
isen	Isentropic

Dimensionless Numbers

Symbol	Explanation	Relation
Gr	Grashof number	$Gr = \dfrac{L^3 g \rho^2 \beta \lvert \Delta T \rvert}{\mu^2}$
Nu	mean Nusselt number	$Nu = \dfrac{\alpha D}{k}$
Pr	Prandtl number	$Pr = \dfrac{\mu C_p}{k}$
Re	Reynolds number	$Re = \dfrac{\rho w D}{\mu}$
Ra	Rayleigh number	$Ra = Gr.Pr$

A 7-point cycle model, shown in figure 2, is chosen to simulate the entire cycle using the refrigerant R134a with two different water reservoir volumes (150L & 200L).
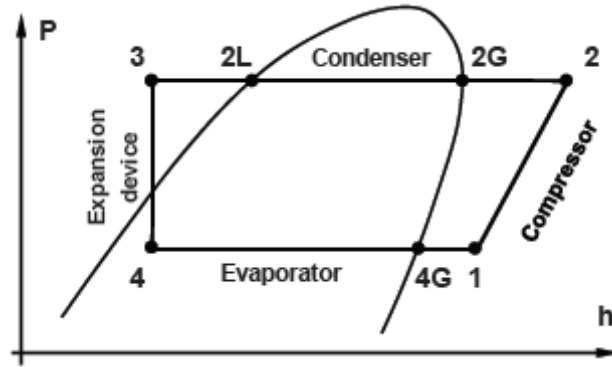

Figure 2: P-h Diagram of the 7-point cycle

2.1 Compressor

There are three key parameters that are of interest in the compressor model. They are compressor mass flow rate ($\dot{m}_k$), outlet enthalpy ($h_{k,out}$), and electrical input power ($\dot{W}_k$), the mass flow rate is given by:

$$\dot{m}_k = \omega_k V_k \rho_k \eta_{vol} \tag{1}$$

Where $\quad \rho_k = \rho(P_{k,in}, h_{k,in}), \eta_{vol} = f_1(P_{ratio}, \omega_k)$

Assuming an adiabatic compression process with an isentropic efficiency, the outlet enthalpy is given by:

$$h_{k,out} = \frac{1}{\eta_k}[h_{k,out,isentropic} - h_{k,in}(1 - \eta_{k,isen})] \tag{2}$$

Where $h_{k,out,isentropic} = h(P_{k,out}, s_{k)}, \; s_k = s(P_{k,in}, h_{k,in})$ and $\eta_{isen} = f_2(P_{ratio}, \omega_k)$

Based on the discharge enthalpy, the compressor useful power ($\dot{W}_k$) is calculated as follows:

$$\dot{W}_k = \dot{m}_k(h_{k,out} - h_{k,in}) \tag{3}$$

2.2 Expansion valve

There are two key parameters expected out of the valve model, the mass flow rate and the outlet enthalpy.
The mass flow rate is given by:

$$\dot{m}_v = C_d\sqrt{\rho(P_{in} - P_{out)}} \tag{4}$$

Where $\quad C_d = \left[\dot{m}_v / \sqrt{\rho(P_{in} - P_{out})} \right]_{nominal}$

Assuming an isenthalpic process, the outlet enthalpy is given by:

$$h_{v,in} = h_{v,out} \tag{5}$$

2.3 Heat exchangers

The dynamics of a vapor compression system are assumed to be dominated by the dynamics of the heat exchangers. The heat exchanger transient models can be generally classified into three groups: lumped parameter models, discretized models, and moving boundary models. In this work, the moving boundary approach is chosen to model both the evaporator and condenser because of its capability to capture important dynamics due to the complex heat exchanger behavior while preserving the simplicity of lumped parameter models.

To derive governing differential equations suitable for simulation, we will begin with the governing partial differential equations (PDEs) for fluid flow in a tube. After applying a few simplifying assumptions, these PDEs can be integrated along the length of the heat exchanger to remove the spatial dependence and yield several ordinary differential equations (ODEs). The assumptions made are: (1) the heat exchanger is assumed to be a long, thin, horizontal tube; (2) The refrigerant flowing through the heat exchanger tube is modeled as a one-dimensional fluid flow; (3) Axial conduction of refrigerant is neglected;(4) Pressure drop along the heat exchanger tube due to momentum change in refrigerant and viscous friction is neglected; thus the equation for conservation of momentum is not needed.

The partial differential equations for conservation of refrigerant mass and energy are illustrated in equations 6 & 7 shown below:

$$\frac{\partial \rho}{\partial t} + \nabla.(\rho \vec{u}) = 0 \tag{6}$$

$$\frac{\partial \rho \left(e + \frac{\vec{u}\vec{u}}{2}\right)}{\partial t} + \nabla.\left(\rho \vec{u}\left(h + \frac{\vec{u}.\vec{u}}{2}\right)\right) = -\nabla.\vec{q} + \rho f \vec{u} + \nabla.(\tau.\vec{u}) + Q \tag{7}$$

Where $\vec{u}$ is the fluid velocity vector, $\vec{f}$ is the body force vector, $\vec{q}$ is heat flux vector, σ is the stress tensor, and τ is the shear stress tensor.

By applying the assumptions outlined previously, these equations are simplified to one-dimensional PDEs illustrated in equations 8 & 9. Additionally an equation for the conservation of heat exchanger wall energy is given in Equation 10.

$$\frac{\partial(\rho A_{cs})}{\partial t} + \frac{\partial(\dot{m})}{\partial z} = 0 \tag{8}$$

$$\frac{\partial(\rho A_{cs}h - A_{cs}P)}{\partial t} + \frac{\partial(\dot{m}h)}{\partial z} = p_i \alpha_i (T_w - T_r) \tag{9}$$

$$\left(C_p \rho A\right)_w \frac{\partial(T_w)}{\partial t} = p_i \alpha_i (T_r - T_w) + p_o \alpha_o (T_a - T_w) \tag{10}$$

Figure 3 shows a schematic of an evaporator. By the phase of refrigerant, an evaporator can be divided into two distinct parts: two-phase region, and superheat region. For the condenser, there is an additional part: subcooled region. lumped parameters are assumed to be associated with each fluid region.
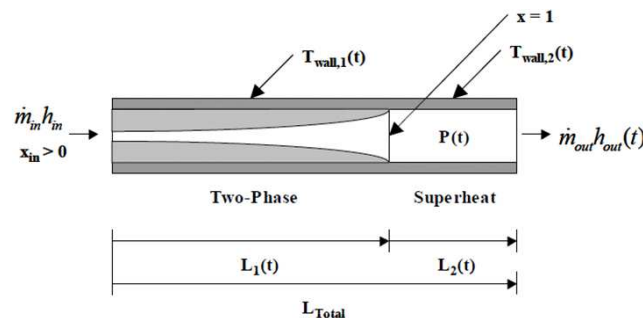

Figure 3: Evaporator with two fluid regions (Rasmussen and Alleyne 2006)

Several assumptions are made regarding the lumped parameters. In the first region, the fluid properties are determined by assuming a mean void fraction. Void fraction is defined as the ratio of vapor volume to total volume, and has long been used to describe certain characteristics of two-phase flows. Thus, $\rho_1 = \rho_f(1 - \bar{\gamma}) + \rho_g(\bar{\gamma})$ and so forth. In the second region, average properties are assumed, i.e. $h_2 = \frac{h_g + h_{out}}{2}$, $T_{r2} = T(P_e, h_2)$, and $\rho_2 = \rho(P_e, h_2)$. The mean void fraction used in this study is found in (Rasmussen and Alleyne 2006):

$$\bar{\gamma} = \frac{1}{b} + \frac{1}{x_2 - x_1}\left[\frac{a}{b}\log\left(\frac{bx_1 + a}{bx_2 + a}\right)\right]$$

Where $a = \left(\frac{\rho_g}{\rho_f}\right)S$ and $b = 1 - a$

x_1, x_2: refrigerant quality at inlet & outlet of two-phase region respectively

The slip ratio S is calculated by Zivi relationship:

$$S = \left(\frac{\rho_f}{\rho_g}\right)^{1/3}$$

Following the Leibniz's integration rule (Rasmussen and Alleyne 2006), equations (8), (9) & (10) can be integrated over each region to give the governing equations for the conservation of refrigerant mass, refrigerant energy, and heat exchanger wall energy respectively.

Conservation of Refrigerant Mass (Two-Phase and Superheated Regions)

$$\frac{d\rho_f}{dP_e}\left(1 - \bar{\gamma} + \frac{d\rho_g}{dP_e}(\bar{\gamma})\right)A_{cs}L_1\dot{P}_e + (\rho_f - \rho_g)(1 - \bar{\gamma})A_{cs}\dot{L}_1 = \dot{m}_{in} - \dot{m}_{int} \tag{11}$$

$$\left[\left.\frac{\partial\rho_2}{\partial\rho_e}\right|_{h_2} + \frac{1}{2}\left(\left.\frac{\partial\rho_2}{\partial h_2}\right|_{P_e}\right)\left(\frac{dh_g}{dP_e}\right)\right]A_{cs}L_2\dot{P}_e + \frac{1}{2}\left(\left.\frac{\partial\rho_2}{\partial h_2}\right|_{P_e}\right)A_{cs}L_2\dot{h}_{out} + (\rho_g - \rho_2)A_{cs}\dot{L}_1 = \dot{m}_{int} - \dot{m}_{out} \tag{12}$$

Conservation of Refrigerant Energy (Two-Phase and Superheated Regions)

$$\left(\frac{d(\rho_f h_f)}{dP_e}(1 - \bar{\gamma}) + \frac{d(\rho_g h_g)}{dP_e}(\bar{\gamma}) - 1\right)A_{cs}L_1\dot{P}_e + (\rho_f h_f - \rho_g\rho_g)(1 - \bar{\gamma})A_{cs}\dot{L}_1 = \dot{m}_{in}h_{in} - \dot{m}_{int}h_{int} + \alpha_{i1}A_i\left(\frac{L_1}{L_{total}}\right)(T_{w1} - T_{r1}) \tag{13}$$

$$\left[\left(\left(\left.\frac{\partial\rho_2}{\partial\rho_e}\right|_{h_2}\right) + \left(\frac{1}{2}\right)\left(\left.\frac{\partial\rho_2}{\partial h_2}\right|_{P_e}\right)\left(\frac{dh_g}{dP_e}\right)\right)h_2 + \left(\frac{1}{2}\right)\left(\frac{dh_g}{dP_e}\right)\rho_2 - 1\right]A_{cs}L_2\dot{P}_e + \left[\left(\left.\frac{\partial\rho_2}{\partial h_2}\right|_{P_e}\right)h_2 + \rho_2\right]\left(\frac{1}{2}\right)A_{cs}L_2\dot{h}_{out} + (\rho_g h_g - \rho_2 h_2)A_{cs}\dot{L}_1 = \dot{m}_{int}h_{int} - \dot{m}_{out}h_{out} + \alpha_{i2}A_i\left(\frac{L_2}{L_{total}}\right)(T_{w2} - T_{r2}) \tag{14}$$

Conservation of Wall Energy (Two-Phase and Superheated Regions)

$$\left(C_p\rho V\right)_w\dot{T}_{w1} = \alpha_{i1}A_i(T_{r1} - T_{w1}) + \alpha_o A_o(T_a - T_{w1}) \tag{15}$$

$$\left(C_p\rho V\right)_w\left[\dot{T}_{w2} - \left(\frac{T_{w2} - T_{w1}}{L_2}\right)\dot{L}_1\right] = \alpha_{i2}A_i(T_{r2} - T_{w2}) + \alpha_o A_o(T_a - T_{w2}) \tag{16}$$

Defining the state vector $x = [\, L_1 \;\; P_e \;\; h_{out} \;\; T_{w1} \;\; T_{w2} \,]^T$ and algebraically combining the equations (11) through (16), the governing equation of evaporator dynamics reduces to the following compact state space form:

$$\begin{bmatrix} z_{11} & z_{12} & 0 & 0 & 0 \\ z_{21} & z_{22} & z_{23} & 0 & 0 \\ z_{31} & z_{32} & z_{33} & 0 & 0 \\ 0 & 0 & 0 & z_{44} & 0 \\ z_{51} & 0 & 0 & 0 & z_{55} \end{bmatrix} \dot{x}_e = \begin{bmatrix} \dot{m}_{in}(h_{in} - h_g) + \alpha_{i1} A_i \left(\frac{L_1}{L_{total}}\right)(T_{w1} - T_{r1}) \\ \dot{m}_{out}(h_g - h_{out}) + \alpha_{i2} A_i \left(\frac{L_2}{L_{total}}\right)(T_{w2} - T_{r2}) \\ \dot{m}_{in} - \dot{m}_{out} \\ \alpha_o A_o (T_a - T_{w1}) - \alpha_{i1} A_i (T_{w1} - T_{r1}) \\ \alpha_o A_o (T_a - T_{w2}) - \alpha_{i2} A_i (T_{w2} - T_{r2}) \end{bmatrix} \qquad (17)$$

Expressions of all elements in matrix [z] are given in the Appendix A.

Similar derivation can be carried out for the condenser dynamics resulting in Equation of the form $[D] * \dot{x}_c = f$, with state vector $x_c = [\, L_1 \;\; L_2 \;\; P_c \;\; h_{out} \;\; T_{w1} \;\; T_{w2} \;\; T_{w3} \,]^T$.

2.4 Water reservoir

The water reservoir stores heated water ready for being supplied to the demand site. The condenser coil is installed inside the water reservoir in a spiral form. As the refrigerant is forced to circulate through the condenser coil, the water temperature in reservoir is raised due to heat rejected from the refrigerant.
For the sake of modeling, several assumptions are made as follows: (1) uniform temperature in the hot water reservoir (stratification is not considered), (2) no external heat loss from the reservoir wall, and (3) the total amount of hot water in the reservoir is conserved (No water consumption during heating process)
It should be noted that the mean water temperature (T_{wat}) is first initialized at the beginning of the calculation procedure, the new value of mean water temperature ($T_{w,new}$) will be calculated from Eq. (18). If $T_{wat,new}$ does not agree with the target hot temperature value, the new value is used in the next step of iteration. This procedure is repeated until T_{wat} reaches a pre-specified value, usually 60℃.

$$T_{wat,new} = T_{wat} + \frac{Q_c * dt}{m_w C_{pw}}$$

2.5 Heat transfer coefficients

The single-phase refrigerant side heat transfer coefficient is computed from the well known Dittus–Boelter correlation:

$$Nu = 0.023 Re^{0.8} Pr^n$$

Where n = 0.4 for heating and n = 0.3 for cooling of refrigerant

The heat transfer coefficient of the two-phase region inside the condenser (Fu et al. 2003) is calculated by the correlations as follows:

$$Nu = 5.03 Re^{1/3} Pr^{1/3} \qquad\qquad \text{if Re < 55000}$$

$$Nu = 0.0265 Re^{0.8} Pr^{1/3} \qquad\qquad \text{if Re > 55000}$$

Where $\qquad$ $Re = \dfrac{0.5.G.\left[1+\left(\rho_f/\rho_g\right)^{1/2}\right]d_i}{\mu_f}$ $\qquad$ and $\qquad$ $G = \dfrac{4\dot{m}}{\pi d_i^2}$

The heat transfer coefficient of the two-phase region inside the evaporator (Granryd et al. 2005) is given by:

$$Nu = 10^{-2}.\left(Re^2 k_f\right)^{0.4}$$

Where $\qquad$ $k_f = \Delta h / L . g$

The water-side natural convection heat transfer coefficient (ASHRAE, 2001) is given by:

$$Nu = 0.13 Ra^{0.33} \qquad\qquad\qquad \text{if} \quad Ra > 10^{\wedge}8$$

$$Nu = 0.56 Ra^{0.25} \qquad\qquad\qquad \text{if} \quad Ra < 10^{\wedge}8$$

The air-side heat transfer coefficient (Fu et al. 2003) is given by:

$$\alpha = 61.67. w_a^{0.63}$$

3 SYSTEM SIMULATION

The purpose of simulating an ASHPWH is to predict the performance of the unit under certain working conditions.

3.1 Input and output parameters

The input parameters shown in table1 are:
1) Geometrical parameters of the heat exchangers.
2) Initial temperatures of water and air.
3) Air flow rate.
4) Water reservoir volume.
5) Compressor theoretical displacement (swept volume).
6) Expansion valve constants
7) Initial state vector in both heat exchangers

The output parameters are:
1) Condensing and evaporating pressures /temperatures.
2) Heating and cooling capacities.
3) Temperature of water in reservoir.
4) Refrigerant mass flow rate of the compressor.
5) Electrical power input to the compressor.
6) Refrigerant mass flow rate of the expansion valve.

Table 1: Simulation Inputs

Parameter	Value	Unit
Degree of super heating	5	°C
Degree of subcooling	5	°C
Initial water temperature	20	°C
Water set temperature	60	°C
Air input temperature	15; 18; 21; 24; 27; 30; 31.5	°C
Volume of water reservoir	200 (150)	L

Mass flow rate of air	0.4	Kg/s
Condenser tube Length	20	m
Condenser tube inner/outer diameters	10/11	mm
Evaporator tube length	12	m
Evaporator tube inner/outer diameters	12/13	mm
Number of compressor cylinders	1	-
Stroke of compressor cylinder	20	mm
Diameter of compressor cylinder	50	mm
Speed of rotation of compressor	29	rps

3.2   Simulation methodology

The most important steps solution algorithm are:
1) Input geometrical parameters.
2) Initialization of state variables.
3) The condensing pressure is updated as a result of the comparison between the mass flow rates of compressor and expansion valve.
4) A backward difference approach is used to calculate the partial derivatives existing in the governing equations.
5) The under-relaxation method is used to achieve convergence.
6) The evaporating pressure is updated in order to control the amount of superheating.
7) Refrigerant properties of are calculated using REFPROP software.

3.3   Results and Discussion

The model is coded into MATLAB simulation program and used to predict system parameters of interest such as hot water temperature, condensing and evaporating pressures, heating capacity, electrical power input and coefficient of performance COP. The figures below show some of the simulated results at 15°C ambient air temperature.
Figure 4 shows the evolution of condensing and evaporating pressures. The condensing pressure rises gradually from the beginning to the end of simulation which is due to the continuous increasing of water temperature.
In figure 5, the input electrical power rises gradually from 400 W to 770 W since the condensing temperature is rising; however, the heating capacity decreases gradually with time.
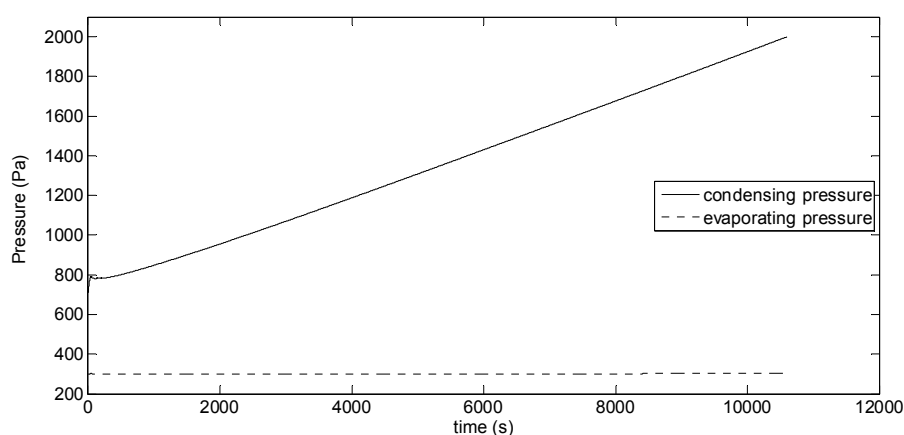

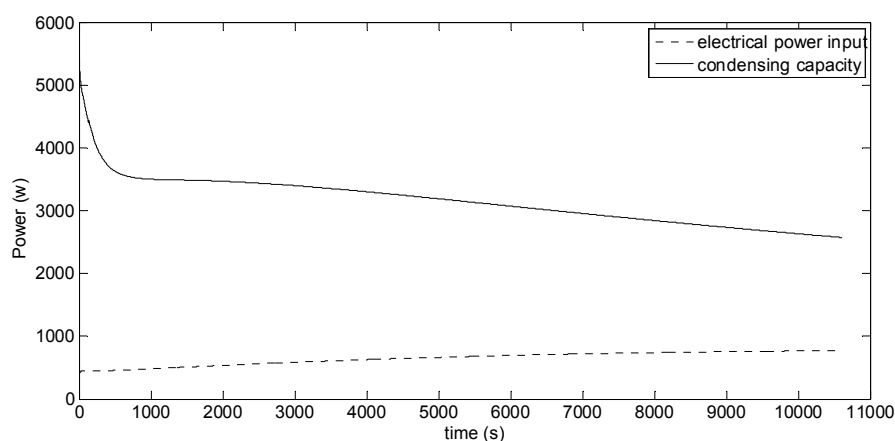**Figure 4: Condensing and evaporating pressures with 200L reservoir**

Figure 5: Heating and input electrical power capacities with 200L reservoir

Figures 6 & 7 present the variations of water temperature in two different water reservoir volumes (150L & 200L). During time progress, the heating energy is rejected to water in the reservoir, and water temperature rises from 20℃ to 60℃. It is obvious that the rate of hot water production increases as the water reservoir volume decreases.
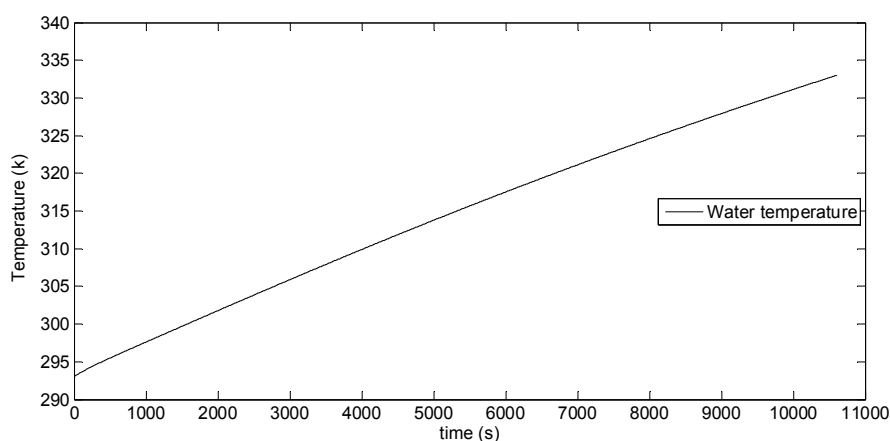

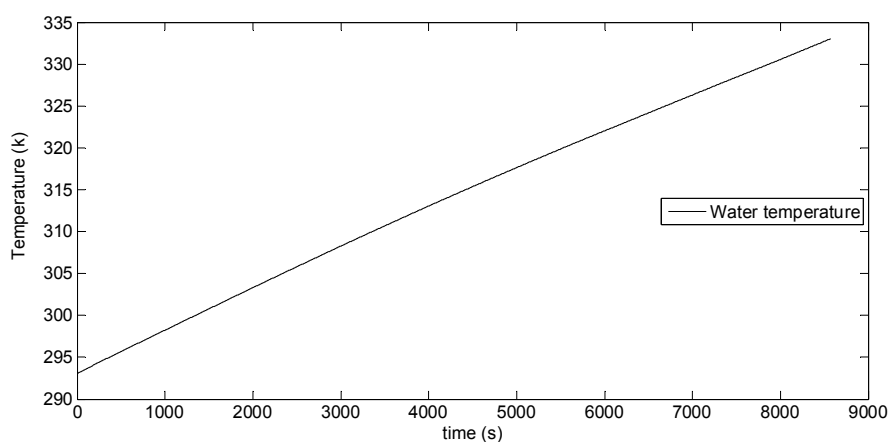**Figure 6: Water temperature with 200L reservoir**

Figure 7: Water temperature with 150L reservoir

Reviewing the meteorological data of Beirut city, which is located in zone 1 of Lebanon, we picked up the hourly ambient dry bulb temperature data over a global year. Analyzing these

data, several ambient temperatures have been chosen to simulate the performance of the ASHPWH corresponding to the integrated COP over a whole reservoir heating cycle.

In figure 8, it is observed that the integrated COP increases as the ambient air temperature increases. Thus, as the ambient temperature rises, more energy can be pumped to the water reservoir and accordingly quite important savings in time and energy are obtained.
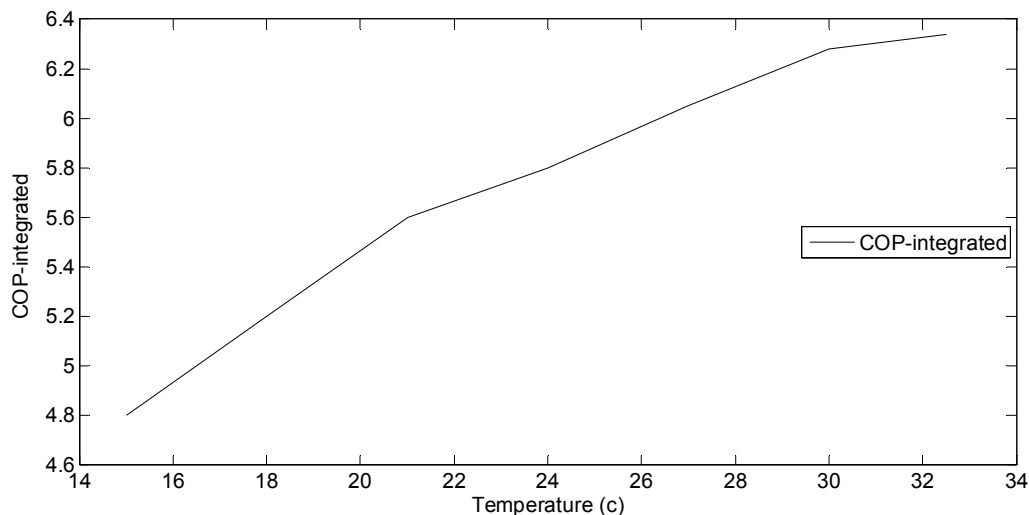

Figure 8: Integrated COP versus ambient temperature

4   Conclusion

A dynamic model for studying the transient characteristics of an air source heat pump water heater (ASHPWH) was developed using MATLAB code. Heat exchangers were modeled by lumped parameter-moving boundary approach while actuator components were modeled by static designs. Based on the developed model, the transient characteristics of the ASHPWH were pressure, temperature, input electrical power, heating capacity and COP, using R134a with two different reservoir volumes (150L & 200L) and at various ambient temperatures . The model was based on fundamental principles of heat transfer, thermodynamics, fluid mechanics, empirical relationships and manufacturer's data as necessary. Simulating the system with the two water reservoir volumes showed that the evolution of all studied parameters were almost the same except for the time needed to reach the pre-specified water temperature (60℃). Moreover, it has been shown that the integrated COP increases as the ambient temperature increases.

Finally, for the selected Lebanese zones (1 & 2), the expected annual value of the integrated COP will vary from 5 to 6 leading to a very high efficiency compared to other hot water production means.

5   References

ASHRAE CD_2001, American Society of Heating, Refrigerating, and Air-Conditioning Engineers.

Chi, J., and D. Didion, Jr. 1982. "A simulation model of the transient performance of a heat pump", International Journal of Refrigeration. 5(3) pp. 176-184.

Fu L., G. Ding and C. Zhang, Jr. 2003. "Dynamic simulation of air-to-water dual-mode heat pump with screw compressor", Applied Thermal Engineering 23 pp. 1629-1645.

Granryd E., I. Ekroth, P. Lundqvist, Â. Melinder, B. Palm, and P. Rohlin, 2005. " REFRIGERATING ENGINEERING", Royal Institute of Technology, KTH, Stockholm

Kapadia R.G., S. Jain, and R.S. Agarwal, 2009. "PhD Transient Characteristics of Split Air-Conditioning Systems Using R-22 and R-410A as Refrigerants", American Society of Heating, Refrigerating and Air-Conditioning Engineers, published in HVAC&R Research, Vol 15, No. 3

Kima M., M.S. Kim, and J.D. Chung, Jr. 2004. "Transient thermal behavior of a water heater system driven by a heat pump", International Journal of Refrigeration 27 pp. 415-421.

MacArthur J.W., E.W. Grald, Jr. 1989 "Unsteady compressible two-phase flow model for predicting cyclic heat pump performance and a comparison with experimental data", International Journal of Refrigeration 12 (1) pp.29-41.

Rasmussen B. P. and A. G. Alleyne 2006. "Dynamic Modeling and Advanced Control of Air Conditioning and Refrigeration Systems", Air Conditioning and Refrigeration Center University of Illinois TR-244

Techarungpaisan P., S. Theerakulpisut, and S. Priprem, Jr. 2007. "Modeling of a split type air conditioner with integrated water heater", Energy Conversion and Management 48 pp. 1222-1237.

UNDP 2005. "CLIMATIC ZONING FOR BUILDINGS IN LEBANON"

Appendix A

$$z_{11} = \rho_f(h_f - h_g)(1 - \bar{\gamma})A_{cs} \quad ; \quad z_{21} = \rho_2(h_g - h_2)A_{cs}$$

$$z_{12} = [(\frac{d(\rho_f h_f)}{dP_e} - \frac{d\rho_f}{dP_e}h_g)(1 - \bar{\gamma}) + \left(\frac{d(\rho_g h_g)}{dP_e} - \frac{d\rho_g}{dP_e}h_g\right)(\bar{\gamma}) - 1]A_{cs}L_1$$

$$z_{22} = \left[\left(\left(\frac{\partial \rho_2}{\partial P_e}\Big|_{h_2}\right) + \left(\frac{1}{2}\right)\left(\frac{\partial \rho_2}{\partial h_2}\Big|_{P_e}\right)\left(\frac{dh_g}{dP_e}\right)\right)(h_2 - h_g) + \left(\frac{\rho_2}{2}\right)\left(\frac{dh_g}{dP_e}\right) 1\right]A_{cs}L_2$$

$$z_{23} = \left[\left(\frac{1}{2}\right)\left(\frac{\partial \rho_2}{\partial h_2}\Big|_{P_e}\right)(h_2 - h_g) + \left(\frac{\rho_2}{2}\right)\right]A_{cs}L_2$$

$$z_{31} = [(\rho_g - \rho_2) + (\rho_f - \rho_g)(1 - \bar{\gamma})]A_{cs}$$

$$z_{32} = \left[\left(\left(\frac{\partial \rho_2}{\partial P_e}\Big|_{h_2}\right) + \left(\frac{1}{2}\right)\left(\frac{\partial \rho_2}{\partial h_2}\Big|_{P_e}\right)\left(\frac{dh_g}{dP_e}\right)\right)L_2 + \left(\left(\frac{d\rho_f}{dP_e}\right)(1 - \bar{\gamma})\left(\frac{d\rho_g}{dP_e}\right)(\bar{\gamma})\right)L_1\right]A_{cs}$$

$$z_{33} = \frac{1}{2}\left(\frac{\partial \rho_2}{\partial h_2}\Big|_{P_e}\right)A_{cs}L_2 \quad ; \quad z_{44} = (C_p\rho V)_w$$

$$z_{51} = (C_p\rho V)_w \left(\frac{T_{w1} - T_{w2}}{L_2}\right) \quad ; \quad z_{55} = (C_p\rho V)_w$$